Journal of Neuroscience Methods 215 (2013) 210–217

Contents lists available at SciVerse ScienceDirect

Journal of Neuroscience Methods

journal homepage: www.elsevier.com/locate/jneumeth

Computational neuroscience

Sample entropy and regularity dimension in complexity analysis of cortical surface structure in early Alzheimer's disease and aging

Ying Chen*, Tuan D. Pham

Aizu Research Cluster for Medical Engineering and Informatics, Research Center for Advanced Information Science and Technology, The University of Aizu, Aizuwakamatsu, Fukushima 965-8580, Japan

HIGHLIGHTS

- A practical model was constructed for calculating SampEn and regularity dimension.
- We applied this model for the first time to quantify brain structural complexity.
- An increase of cortical surface structure complexity was detected in early AD.
- An increasing structural irregularity with aging was observed.
- The model may be used to construct a useful biomarker of AD and cognitive decline.

GRAPHICAL ABSTRACT

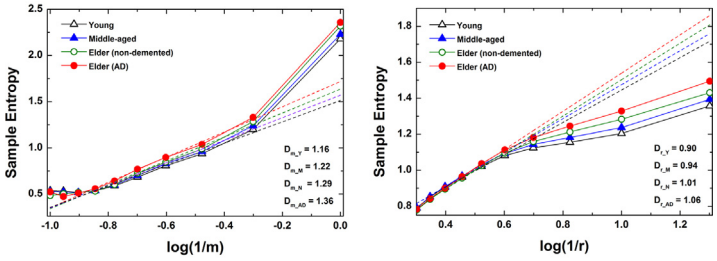

ARTICLE INFO

Article history:
Received 15 December 2012
Received in revised form 21 March 2013
Accepted 22 March 2013

Keywords:
MRI
Regularity dimension
Sample entropy
Alzheimer's disease
Aging

ABSTRACT

We apply for the first time the sample entropy (SampEn) and regularity dimension model for measuring signal complexity to quantify the structural complexity of the brain on MRI. The concept of the regularity dimension is based on the theory of chaos for studying nonlinear dynamical systems, where power laws and entropy measure are adopted to develop the regularity dimension for modeling a mathematical relationship between the frequencies with which information about signal regularity changes in various scales. The sample entropy and regularity dimension of MRI-based brain structural complexity are computed for early Alzheimer's disease (AD) elder adults and age and gender-matched non-demented controls, as well as for a wide range of ages from young people to elder adults. A significantly higher global cortical structure complexity is detected in AD individuals ($p < 0.001$). The increase of SampEn and the regularity dimension are also found to be accompanied with aging which might indicate an age-related exacerbation of cortical structural irregularity. The provided model can be potentially used as an imaging bio-marker for early prediction of AD and age-related cognitive decline.

1. Introduction

Normal aging was accompanied by a gradual loss of neurones, whereas demented brains showed a much more severe decrease (Ball, 1977). Cognitively normal brain shows age-related changes that include an overall reduction in brain volume and weight, which are associated with gyral atrophy and widening of the sulci of the cerebral cortex, and enlargement of the brain ventricles. Dementia is an age-related cognitive decline which is indicated by an early degeneration of cortical and sub-cortical structures (Rogan and Lippa, 2002; Fotenos et al., 2005). Alzheimer's disease (AD), the most common cause of dementia, has shown to be characterized by an insidious onset of cerebral atrophy and reduced gray matter (GM) over the whole brain (Fox et al., 1996; Sluimer et al., 2008; Spulber et al., 2012), and within specific anatomical regions

* Corresponding author. Tel.: +81 242 37 2568; fax: +81 242 37 2568.
E-mail addresses: ychen@u-aizu.ac.jp (Y. Chen), tdpham@u-aizu.ac.jp (T.D. Pham).

0165-0270/$ – see front matter © 2013 Elsevier B.V. All rights reserved.
http://dx.doi.org/10.1016/j.jneumeth.2013.03.018

such as frontal (The Lund and Manchester Groups, 1994; Burton et al., 2002; Thompson et al., 2003), temporal (Whitwell et al., 2007; Hamalainen et al., 2007), parietal (Whitwell et al., 2007; Im et al., 2008b) and hippocampal cortex (Shi et al., 2009; Whitwell et al., 2007) compared to normal controls. Meanwhile, there is also a strong genetic contribution to developing the disease at least implies that it may not be the inevitable, even if frequent, consequence of old age.

As a non-invasive tool, advanced brain imaging can be especially superior in early prediction and also allows medical researchers to observe details and to match morphological changes in the physical structure of the brain to changes in cognitive performance over time (Davidson and Heinrichs, 2003; Toulopoulou et al., 2004; Glei et al., 2005). The ability to accurately distinguish or classify closely related objects is even more useful for practical purposes. Recent magnetic resonance (MR) morphological studies enable the measure of voxel-based differences in GM volume (Burton et al., 2002; Giulietti et al., 2012), density (Hamalainen et al., 2007), and cortical thickness (Dickerson et al., 2009; Im et al., 2008b). Volumetric characterization, however, is one of the many aspects of human anatomical structure. There is also other information not available by volumetric analysis that may be gained using other analysis techniques. Brain structural variability can be a useful indicator for identifying clinically relevant information on neuroimaging scans. It can be captured by measuring brain complexity and calculating the fractal dimension, which measures the complexity of sulcal anatomy in an analogous way to measure the folding of the cortex (Zhang et al., 2008). Brain structural complexity is reported to be highly variable across different ages (Kochunov et al., 2005), between men and women (Luders et al., 2004), and in brain-related disorders such as schizophrenia (Sandu et al., 2008), stroke (Zhang et al., 2008), cerebellar degeneration (Wu et al., 2010), and Alzheimer's disease (King et al., 2010).

The quantification of the complexity of image patterns is helpful because it provides us an insight into the mechanism and characteristics of a particular complex system in order to advance our understanding or confirm our hypothesis of the problem under study. The entropy measure provides a way to study the system complexity by quantifying the geometry structures. Within the entropy family, approximate entropy (ApEn) and its modified methods have been introduced for studying regularity and complexity in physiological and biological time-series (Pincus, 1991a). ApEn quantifies the conditional probability that two sequences similar for m points (within a given tolerance r) remain similar when one consecutive point is included. Sample entropy (SampEn) is an improved algorithm of ApEn (Richman and Moorman, 2000) which avoids the bias caused by self-matching. Multi-scale entropy (MSE) uses SampEn to quantify the regularity of data by taking into account multiple time scales. All above measures depend on the selection of the two parameters known as m and r. The regularity dimension (Pham, 2012) has been recently introduced as a novel model for measuring signal complexity. It was developed for modeling a mathematical relationship between the frequency with which information about signal regularity changes in various scales. In that sense, it can be used as a tool to unify the entropy-based variety subject to different values of m and r. This quantification is very useful for studying various types of biosignals, and has been successfully applied for phylogenetic tree reconstruction of mitochondrial DNA sequences (Pham, 2012). SampEn has been applied in EEG data to discover a loss of complexity in AD patient, indicating a destruction of nonlinear structures in brain dynamics (Abasolo et al., 2006). But it is not clear whether this abnormalities of complexity can be also detected in cortical anatomy of demented subjects and be reliably measured across different subject samples.

In the present study, we applied the sample entropy and regularity dimension to characterize the MRI-based cortical surface structural complexity in subjects with early AD and non-demented elders. We aimed to answer the question whether this new measure of brain structural complexity can distinguish the difference of who were with and without AD, and if so, how it is associated with AD. Furthermore, we estimated the sample entropy and regularity dimension over a wide range of ages from young to elder adults to study the age-related development of brain structural complexity. We aimed to construct a practical model to calculate the sampled entropy and regularity dimension based on MRI data, and prove the feasibility of these new measures as an imaging bio-marker for early prediction of AD and age-related cognitive decline.

2. Sample entropy and regularity dimensions

For a given time-series $X = x_1, \ldots, x_N$, its SampEn can be calculated by the following equation (Richman and Moorman, 2000):

$$\mathrm{SampEn}(m, r, N) = -\ln\left[\frac{A^m(r)}{B^m(r)}\right] \tag{1}$$

where m is the length of sequence to be compared (also known as embedded dimension), N is the length of the input series, and r is the tolerance for accepting matches. $B^m(r)$ is the probability that two sequences will match for m points, whereas $A^m(r)$ is the probability that two sequences will match for $m+1$ points. The algorithm builds up runs of points matching within the tolerance r until there is not a match, and keeps track of template matches continued until the end of the data.

The idea of regularity dimension is based on the concept of power laws and entropy measures. For the scaling exponent in power law constructs, an empirical rule is that the number of increments is proportional to a scale size raised to some power. That means the slope of the best-fit straight line in the logarithmic plot is the exponent which is called the dimension. In that sense, dimension is considered as an important mathematical characteristic because it can quantify the rate of change between the number of increments and the corresponding varying scale size.

The general rule of the power or exponent dimension can be expressed in terms of a power law as

$$\Delta \propto s^{-D} \tag{2}$$

where Δ, $\propto$, s and D stand for the number of increments, proportional to, scale size, and exponent dimension, respectively.

We can rearrange (2) to obtain the exponent dimension as

$$D \propto \frac{\log(\Delta)}{\log(1/s)} \tag{3}$$

Based on the expression of (3), the regularity dimension can be derived by entropy measures, here we used SampEn.

It has been known that information (such as SampEn) increases with decreasing size of the lag space (Williams, 1997) such as m in this case. In other words, the information is approximately proportional to the log of $1/m$. A straight line of the semilog axes is therefore expected in a plot of $1/m$ versus I, and the mathematical relation is a logarithmic equation. Because the relation is a straight line, it has the following form:

$$I_m = a + D_m \log\left(\frac{1}{m}\right) \tag{4}$$

where I_m is SampEn denoting the information subject to m, a is a constant which is the intercept, and D_m is the slope of the straight line, which is also the regularity dimension.

Table 1
Subjects information.

	Young	Middle-aged	Elder (non-demented)	Elder (AD)
Number	52	52	52	52
Sex (female/male)	26/26	26/26	26/26	26/26
Age (years)	22.7 ± 3.4 (18–29)	42.4 ± 6.8 (30–51)	75.4 ± 8.6 (61–90)	75.6 ± 7.4 (63–92)
CDR	0	0	0	0.5 or 1

Values given are mean ± SD. Values in parentheses represent the range.

Rearrangement of (4) We can get

$$D_m = \frac{I_m}{\log(1/m)} - \frac{a}{\log(1/m)} \tag{5}$$

Setting a limit term on m, which indicates that the relation does not hold for very large m, gives

$$D_m = \lim_{m\to 0} \frac{I_m}{\log(1/m)} - \frac{a}{\log(1/m)} \tag{6}$$

Since a is a constant, the term $a/[\log(1/m)]$ approaches zero in the limit of m approaching zero, and therefore this term becomes negligibly small. Thus, (6) can be simplified as

$$D_m = \lim_{m\to 0} \frac{I_m}{\log(1/m)} \tag{7}$$

It can be noted from (7) that the regularity dimension D_m measures the rate of change of signal regularity/predictability with respect to $\log(1/m)$, and it is the rate at which the entropy of a dynamical system is gained with increasing resolution (decreasing length m).

Alternatively, increasing the value of r, which is the tolerance of similarity, decreases the information in the sense that no information is gained when most subsequences are considered to be similar (signal is highly predictable or has low complexity). Being analogous to the relation of a straight line developed for D_m, the regularity dimension D_r can be obtained as

$$D_r = \lim_{r\to 0} \frac{I_r}{\log(1/r)} \tag{8}$$

where I_r is SampEn denoting the information subject to r.

3. Experiment

3.1. Subjects

All subjects were drawn from the Open Access Series of Imaging Studies (OASIS) database (http://www.oasis-brain.org) (Marcus et al., 2007). From the database, we selected a data set consisting of a cross-sectional collection of young, middle-aged, non-demented and AD elder adults (Table 1). The subjects were all right-handed and included both men and women. 52 of the included subjects had been clinically diagnosed with very mild to mild AD (with Clinical Dementia Rating (CDR) score of 0.5 or 1); and others with CDR score of 0. All studies were approved by the Institutional Review Board (IRB) of Washington University. Informed consents were obtained from all subjects at the time of study participation.

3.2. MRI data pre-processing

All images were corrected for inhomogeneity prior to further segmentation. For each subject, the following images are provided, including: (1) 3–4 individual images corresponding to multiple repetitions of the same structural protocol within a single session to increase signal-to-noise, (2) an average image that is a motion-corrected co-registered average of all available data, (3) a gain-field corrected atlas-registered image to the 1988 atlas space of Talairach and Tournoux (Buckner et al., 2004), (4) a masked T88 image in which all non-brain voxels have been set to 0, and (5) a gray/white/CSF segmented image (Zhang et al., 2001) in which each voxel has been labeled as GM, white matter (WM), or CSF. In the present study, the segmented images provided by the database were used for analysis. All images are in 16-bit big-endian Analyze 7.5 format, and are normalized into $176 \times 208 \times 176$ voxel-wise images. Additional details of the image characteristics can be found at (http://www.oasis-brain.org) (Marcus et al., 2007).

3.3. Generating time series

In order to generate 1-D signals that allow the application of estimating SampEn and regularity dimension, the surface structure of the GM should be represented by time-series. For each transaction, the time series represent the distances measured from subsequent outer boundary points to the GM center of mass; the distances are measured within each single MR slice (in a 2-D plane); one MR slice yields one time series. The whole cortical surface structure is then represented by 130–140 time series extracting from their corresponding MR image slices. Cognitive decline cannot always be reflected in the alterations of folding shapes, but sometimes initiates from imperceptible shrink, dilation, twist or distortion. By depicting the distances between the boundary points and the GM center of each cortical sheet, we were able to build up time-series that can best reflect the micro-structures of the cortical surface architecture including its folding patterns and any shape changes, and as thus enable complexity analysis.

The center of the GM was detected by using the Matlab function called “regionprops” which calculates the centroids of the image regions labeled in the matrix of a two-dimensional array of non-negative integers that represent contiguous regions. Each centroid is 1-by-n dims vector that specifies the center of mass of the region. The location of the boundaries of GM in each 2-D scan was carried out by using the Matlab function called “bwtraceboundary” which traces the outline of an object in a binary image. All these functions are available in the Matlab Image Processing Toolbox. Fig. 1 presents typical examples of detected boundary contour of the GM and its corresponding generated time-series.

3.4. Estimating regularity dimensions from sample entropy

In the present study, regularity dimension D_m was calculated with a fixed r at 0.1 and m varies from 1 to 10, whereas regularity dimension D_r was estimated with a m fixed at 2 while r increased from 0.05 to 0.5 with an interval of 0.05. Regularity dimension for each group was estimated in two ways. In the first way, for each individual, SampEn was calculated with varied pairs of m and r for each time-series, and then averaged over the whole brain. Regularity dimension was estimated based on averaged SampEn. Thereupon we got one regularity dimension D_m and D_r for each individual that can be compared among groups. The other way was that, after obtaining the SampEn for each individual, we averaged SampEn further for the whole group. The regularity dimension was estimated based on the averaged SampEn and we got a single value of D_m and D_r for each group.

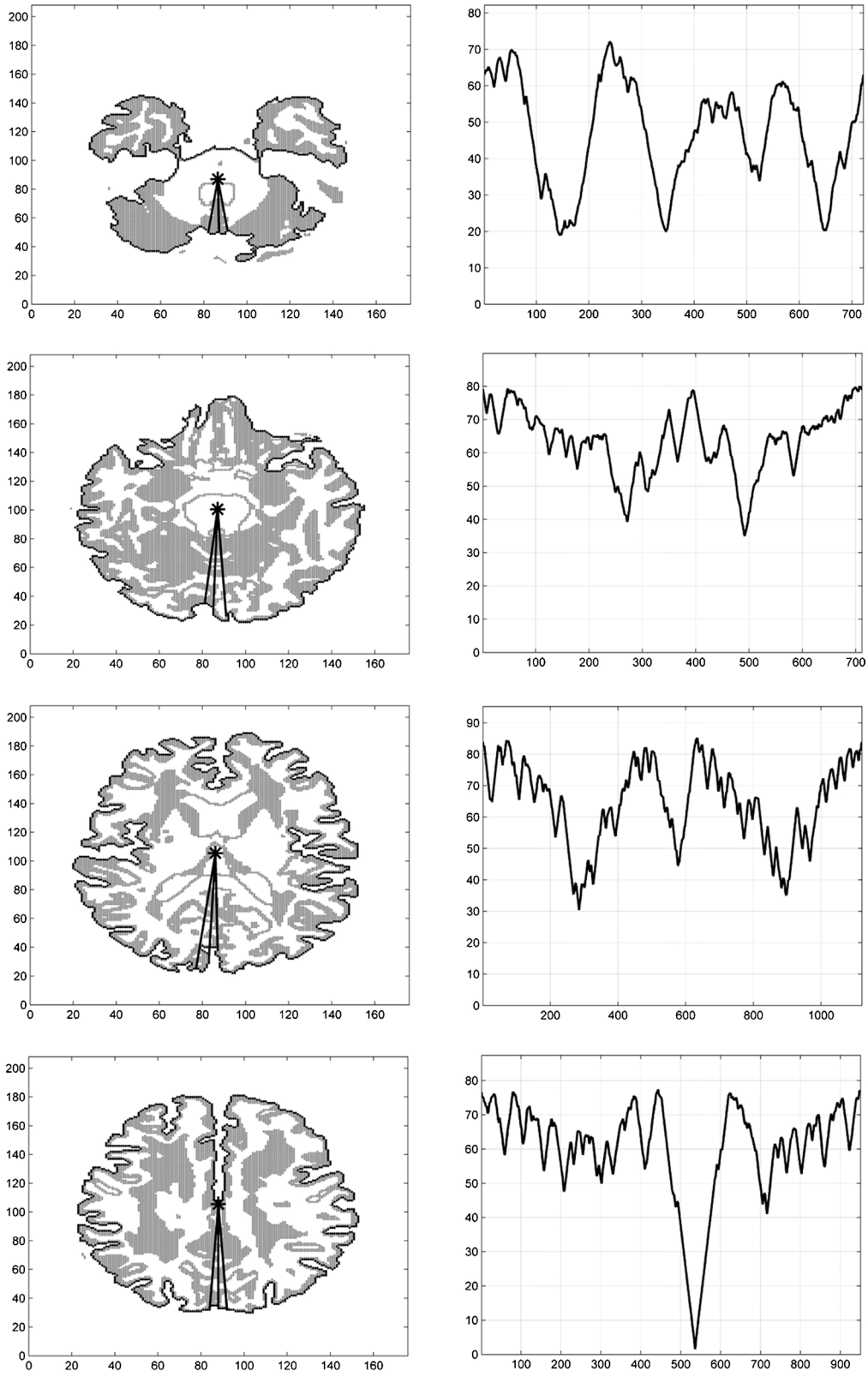

Fig. 1. Typical examples of detected boundary contours (black) of the gray matter (gray) (left) and the corresponding generated time-series (right), where in (right), the time series indicates the distances measured from the gray matter center to subsequent outer boundary points.

Regularity dimension was compared among groups by using ANOVA analysis, and the two independent samples *t*-test was applied to compare the level of differences in regularity dimension between each two groups. The significance level was set to $p < 0.05$.

4. Results

Fig. 2 shows how SampEn varied with *m* and *r*. The slope of the best-fit straight line in the logarithmic plot is the expected regularity dimension.

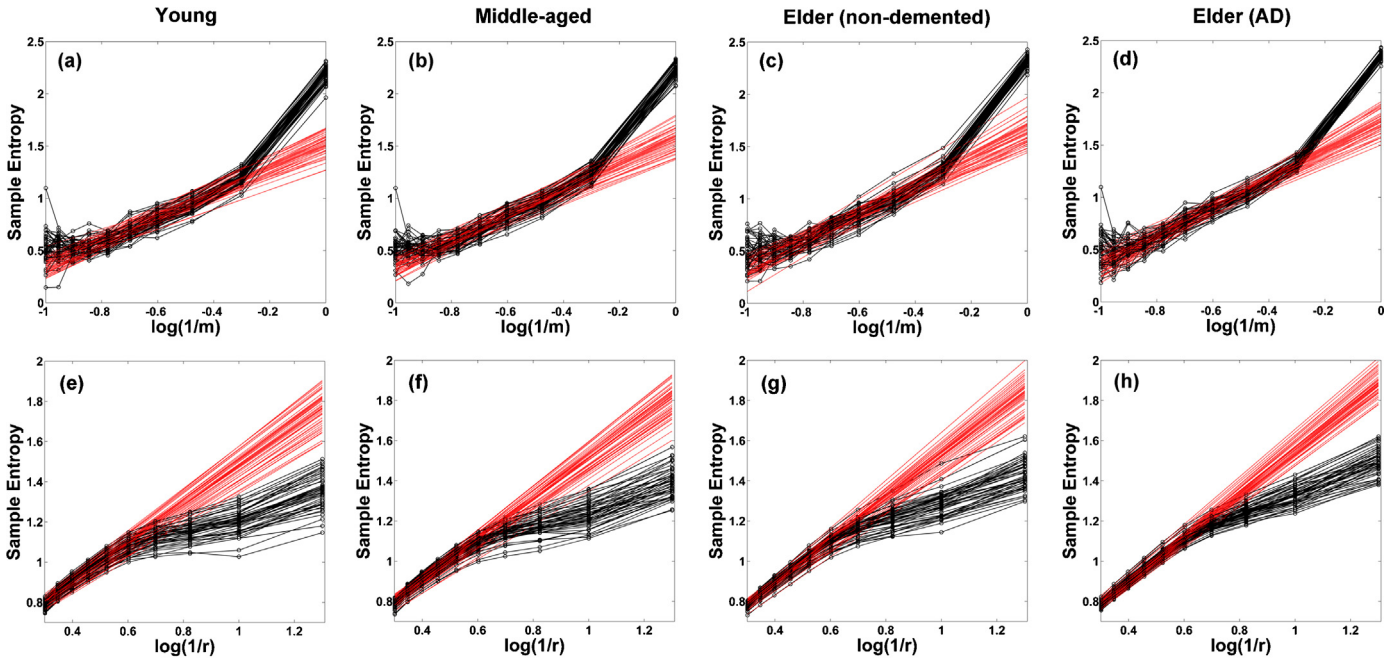

Fig. 2. For each plot, symbols and curves in black are the calculated SampEn with changing m(a–d), or r (e–h) for each individual. The slopes of the best-fit straight lines in red are the expected D_m (a–d) or D_r (e–h). (For interpretation of the references to color in this figure legend, the reader is referred to the web version of the article.)

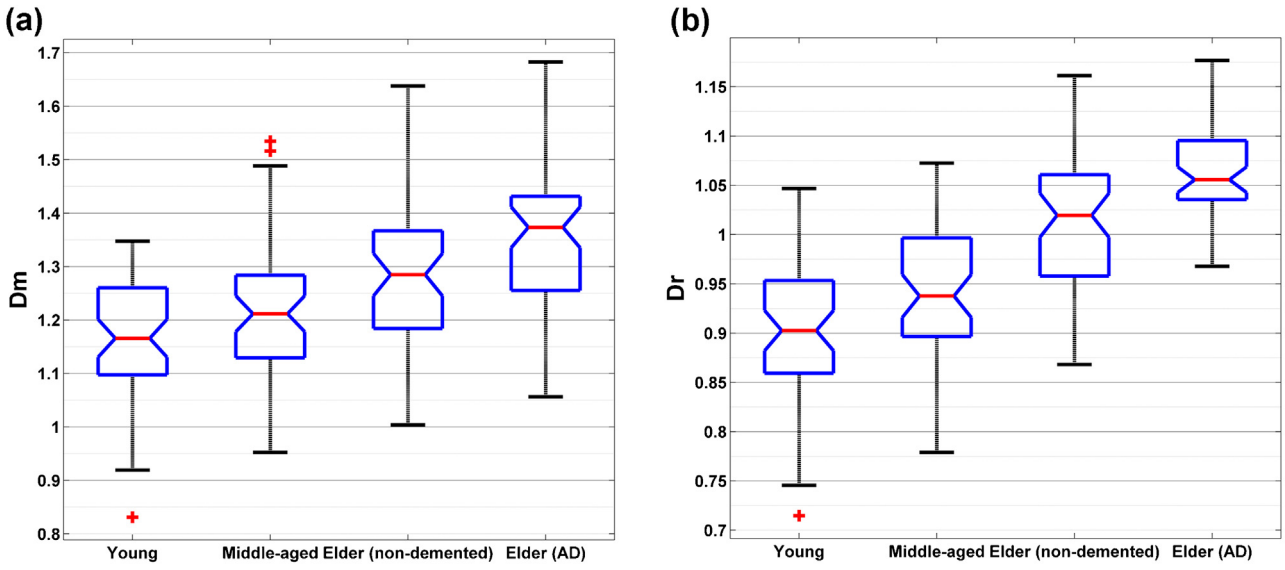

Fig. 3. Box-and-whisker plots of regularity dimension D_m (a) and D_r (b) for the four groups. Outliers indicated as "+".

Fig. 3 shows the box-and-whisker plot of the regularity dimension D_m and D_r for each group. Box-and-whisker plot was used to graphically depict the profiles of regularity dimension: the lower limit of 95% confidence interval, lower quartile, median, upper quartile, and upper limit of 95% confidence interval. Mean values of D_m and D_r were listed in Table 2.

4.1. Distinguish between non-demented and AD subjects

From Fig. 3, AD group was found to have much higher median values in both D_m and D_r than non-demented ones. Mean D_m and D_r are higher in AD individuals compared to non-demented ones as shown in Table 2. This result is in accordance with averaged SampEn ($m = 2$, $r = 0.1$) which is smaller in non-demented individuals. Two independent samples t-test show a highly significant difference ($p < 0.001$) between non-demented and AD subjects (Table 3).

Table 2
Sample entropy and regularity dimension for each group.

	D_m	D_r	Sample entropy
Young	1.16 ± 0.12	0.90 ± 0.07	1.20 ± 0.06
Middle-aged	1.22 ± 0.13	0.94 ± 0.07	1.24 ± 0.06
Elder (non-demented)	1.29 ± 0.15	1.01 ± 0.07	1.28 ± 0.06
Elder (AD)	1.36 ± 0.15	1.06 ± 0.05	1.33 ± 0.05

Values given are mean ± SD.

Table 3
Results of statistical comparisons among groups.

	D_{m_Y}	D_{m_M}	D_{m_N}	D_{m_AD}
D_{m_Y}				
D_{m_M}	*			
D_{m_N}	**	*		
D_{m_AD}	**	**	**	

	D_{r_Y}	D_{r_M}	D_{r_N}	D_{r_AD}
D_{r_Y}				
D_{r_M}	*			
D_{r_N}	**	**		
D_{r_AD}	**	**	**	

Y, M, N and AD refer to young, middle-aged, non-demented and AD, respectively.
*Significant difference at $p < 0.05$.
**Significant difference at $p < 0.001$.

4.2. Age-related changes in cortical surface structural complexity

Fig. 3 shows an increasing tendency of regularity dimension accompanied with aging. Computed results of D_m and D_r were listed in Table 2. Young individuals seem to have more regular cortical surface structure, while structural complexity increases in middle-aged and elder subjects. This increasing tendency in regularity dimension was also in accordance with the results of SampEn as shown in Table 2. The differences were proved to be statistically prominent between each two groups (Table 3).

SampEn was averaged over all individuals in each group, and its relationship with varied m or r was presented in Fig. 4. Regularity dimension D_m and D_r were estimated based on the best-fit straight line of the curve. The computed D_m and D_r show similar results as the D_m and D_r averaged from each individual shown in Table 2 suggested that this method was robust to noise and reliable in practical application. The fact that regularity dimension increased with aging and was significantly higher in AD individuals might indicate an age-related cognitive decline.

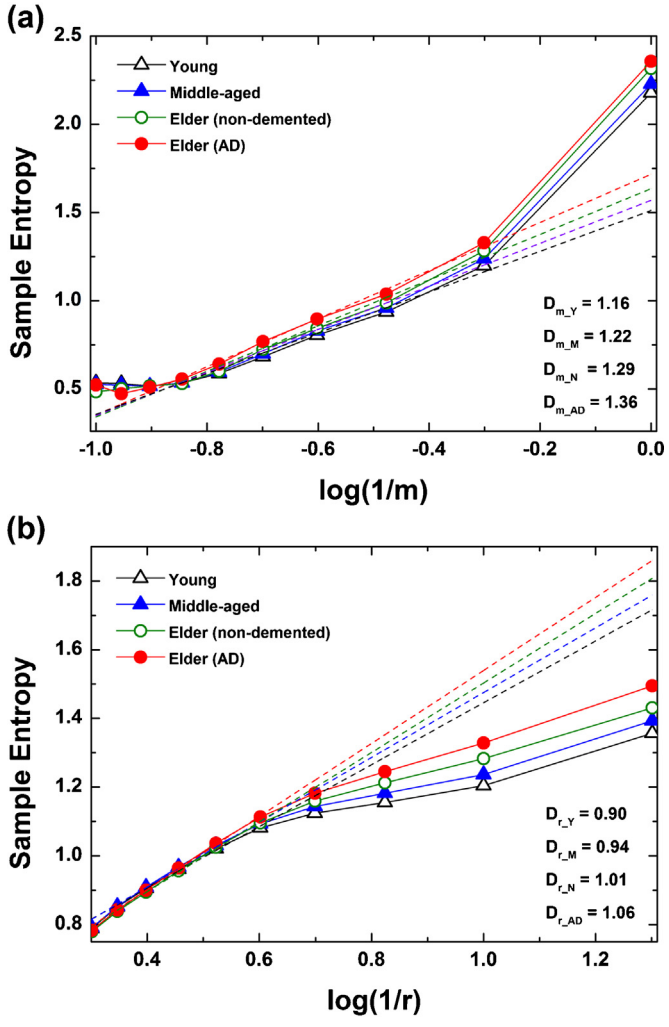

Fig. 4. Regularity dimension for the four groups. Solid lines and symbols show the relationship between averaged SampEn and varied m (a) and r (b). Dashed lines are the corresponding best-fit straight lines. D_m and D_r are estimated by computing the slopes of the straight lines.

5. Discussion

In the current study, significant higher SampEn and regularity dimension obtained from subjects at early stage of AD indicated an increase of irregularity in the cortical surface structure, which might be the result of the reduction in GM volume. The declination of global GM volume has been reported to be associated with cognitive function (Whitwell et al., 2007). Such loss of brain tissue most likely resulted in a shrinking of the surface with an increase in cortical boundary irregularity (as the volume is reduced). This morphological abnormalities can be also associated with the structural changes in cortical sulci. A phase- and region-specific cortical thinning, sulcal widening and shallowing were detected previously by using quantitative surface-based methods in AD patients (Im et al., 2008a,b) and shown to be age-related (Kochunov et al., 2005). However, it should be noted that, greater SampEn and regularity dimension did not particularly indicate the increases in cortical micro-folding, since they did not take gyri and sulci specifically into consideration, but quantified the whole surface into much more detailed structures and evaluated the degree of its self-similarity. Any imperceptible morphological changes can contribute to the variations in boundary complexity. We also found the age-related progressing in cortical structural irregularity. This supports previous MRI-volumetric observations that cortical atrophy occurred before the onset of dementia (from normal to CDR = 0.5), progressed with aging, and accelerated once dementia starts (Good et al., 2001; Im et al., 2008b). We depicted a profile of the increasing complexity in cortical surface structure from young health to clinically healthy elders, then to clinically diagnosed AD (Figs. 3 and 4). Particularly, we detected a significant difference between elder dements and their age- and gender-matched controls. This demonstrated acceleration of brain aging in those elder demented individuals which align with the concept of progressive neurodegeneration in AD individuals. Alzheimer's disease may exhibit a characteristic pattern of atrophy different from that due to aging, even accelerated aging. Studies of other added effect of Alzheimer's over aging have been done by several groups on GM atrophy patterns, for example, the different behavior of hippocampus atrophy versus whole-brain atrophy over the course of the disease (Shi et al., 2009; Whitwell et al., 2007). However, due to the limitation of the data provided by OASIS database which does not include younger dementia subjects, we are not able to further prove whether this severe decrease of cortical structural regularity is simply the inevitable outcome of accelerated aging or if it is exceeding that of controls at any age. This issue is certainly worth investigating in our future research when more data become available.

Regarding the large variances and the overlapping observed from Fig. 3, two possible reasons may explain why we cannot get clear-cut differences between different groups. In the first part of the study, we investigated cortical surface structure in the dementia and controls. As we know AD is a slowly progressive disorder, which is a more sensitive indicator of the severity of brain insult required before cognitive networks change. That means, certain damage can be developed and sustained before reaching a threshold for clinical expression. There is a concept called "cognitive reserve" (Stern, 2002). For demented individuals, a more regular cortical structure (with small SampEn and regularity dimension) might result in a clinical deficit due to less

brain reserve capacity (BRC). On the contrary, for normal subjects, individuals with greater cortical structure irregularity (with large SampEn and regularity dimension) could remain unaffected, because this threshold is not exceeded. In our study, only very mild AD subjects were included, which increases the incidence of this overlapping. In order to see a clear-cut difference, the provided approach needs to be further validated in moderate and severe AD cohorts. The second part of this study addressed the cortex structural changes with normal aging. Being different to dementia, these changes result from inherent physiological rhythms but not disease (Anderton, 1997). Subjects included here were not specially designed for age study, but widely distributed and simply sorted to different age spans. Each span has an age difference varied from 11 years to 30 years. This can explain why there was large variance and overlaps within and among groups. However, it can be noticed that, the overlapping became less when age differences increased.

Extracted features using the concepts of entropy, fractals and chaos to study shapes and functions of the brain have been shown more effective than other features (Liebovitch, 1997; Goldberger et al., 2002). However, some descriptors suffer from several simplified assumptions and restrictions, which make them far from distinguishing different complex patterns. Experimental data are inevitably contaminated by noise in various degrees, straightforward use of these descriptors may not give a clear interpretation of closely related entities because the computation assumes that image models are noise-free or objects of interest are manually extracted. SampEn is proved to be useful in the study of the complexity of short and noisy biological time series (Richman and Moorman, 2000). Unlike some other measures that are time consuming and operator dependent and therefore not always practical in a clinical settings, SampEn shows fast, validated and robust to noise (Pincus, 1991b; Richman and Moorman, 2000), and may have particular advantages when it comes to widespread uptake in either clinical or research practice.

SampEn provides a way of quantifying the shape complexity of objects into a single numerical value, which can be compared between groups of patients, or between patients and healthy controls. However, since we normally have no a priori knowledge concerning the dimension of a system, it is imperative that we evaluated the method for different m and r. Regularity dimension provides a approach to unify multiple solutions due to the choice among the varieties of the values of entropy parameters m and r. It is an abstract space in which small changes in a variable can be tracked and quantified, thus makes it suitable for the dynamic analysis of complex sequential data. We found in the present study that the obtained results generally agree with that obtained from established methods (SampEn), and shows much more sensitivity than SampEn to reflect the differences (Table 2). Since regularity dimension unified the information of entropy with various scales, it takes advantage of all the available data and is more robust to changes in embedding dimension, size of data set, and noise level.

Because it was the first time to apply SampEn and regularity dimension to study the structural MR images, before the research, we tested the validation of both methods in a larger data set from OASIS including 96 demented and 96 age and gender matched non-demented subjects. The two methods were applied successfully in discriminating the two groups. In addition, considering the number of data points in a time-series depends on the circumference of the cortex which differs throughout the whole brain. To exclude the influence of the length of the time series, we clustered all the slices of each MR image into five sub-sections as ~30 layers, 41–60 layers, 61–80 layers, 81–120 layers, and 121~ layers from top to bottom. The computed SampEn and regularity dimension was then compared between the two groups for each sub-section. Results showed in accordance throughout the whole brain that demented subjects have higher SampEn and regularity dimension in all the sub-sections. Specifically, a significant difference at $p < 0.05$ was detected in the middle four sub-sections.

A fundamental problem in implementing regularity dimension was how to generate the time-series from a 3-D model that can best reflect the morphological characteristics. Conventional methods like box-counting method and Minkowski–Bouligand use boxes or spheres to measure the object (Sandu et al., 2008). Here, we constructed the time-series by extracting the distances measured from subsequent outer boundary points to the GM center of mass. The choice of the time series is not arbitrary but carefully based on the structural characteristics of the cortical surface. Sulcal folds are the principal surface landmarks of the human cerebral cortex, and exhibit structurally complex patterns (Welker, 1990) that are postulated to reflect underlying connectivity (Van Essen, 1997). In addition to cortical folding patterns, fractal properties or other irregularities of the cortex architecture arises secondary to the folding of the cortex may also provide information for the developmental events (Sandu et al., 2008; Zhang et al., 2008; King et al., 2010; Liu et al., 2012). Unlike other methods mentioned above simply used for the folding studies, the distances between the boundary points and the GM center can depict and capture the architectural feature of the cortex surface including its gyrification, sulcal span, folding, fractal, and can be sensitive to any imperceptible pattern changes. Because the whole cortical surface structure is represented by 130–140 time series extracting from their corresponding 2-D MR image slices, we are therefore able to evaluate the overall structural complexity for the whole cortical surface.

A practical model was constructed for calculating regularity dimension in the current study which was proved as a potential indicator to predict cognitive impairment even at very early stage. However, there are still some limitations, e.g. it does not allow phase- and region-specific study. Thus, whether this increase of cortical surface structure irregularity is region-specific or an overall abnormality still needs further investigation. Since only very mild and mild AD were included in this study, how it developed in moderate and severe stage of AD will need to take more subjects into study. Depending on the handling by the segmentation method of CSF-GM partial volume voxels on the cortical outer boundary, the outer brain boundary would appear to be either less regular (if narrow sulci are segmented as non-brain voxels, introducing a new boundary with shorter distances to the GM center of mass) or more regular (if narrow sulci are segmented as brain voxels, leaving the boundaries of those sulci as part of the brain tissue and not representing them in the time series). Meanwhile, we have noticed that some WM hyper-intensities were classified as GM, especially the boarder voxels between GM and WM, and possibly the GM center of mass may be influenced by the presence of the WM hyper-intensities. Due to the limitation of the segmentation and boundary tracing method, some potential sensitivity of the approach is probably lost. To overcome above limitations, more detailed segmentation and boundary tracing method should be applied to future study, such as that provided by the SPM or FreeSurfer sofware.

6. Conclusion

We have demonstrated the increase of global cortical surface structure complexity in early AD. The results suggest that such abnormalities are an important and salient characteristic of patients at the early stages of cognitive impairment. We also found an increasing cortical structural irregularity with aging which might contribute to the age-related cognitive decline. The provided model using SampEn and regularity dimension can be used as computer-aid tool for validating imaging bio-markers of AD and

age-related cognitive impairment and could thus potentially aid in the timely and accurate clinical diagnosis of disease. Current results also pave way for our future studies which aim to combine the use of SampEn, regularity dimension and other features to build up a MRI-based model for individual classification and early prediction of cognitive impairment.

Acknowledgment

This work was supported by JSPS Grants-in-Aid for Scientific Research (Research Activity Start-up) awarded to Tuan D. Pham.

References

Abasolo D, Hornero R, Espino P, Alvarez D, Poza J. Entropy analysis of the EEG background activity in Alzheimer's disease patients. Physiol Meas 2006;27:241–53.
Anderton BH. Changes in the ageing brain in health and disease. Philos Trans R Soc Lond B: Biol Sci 1997;352(1363):1781–92.
Ball MJ. Neuronal loss, neurofibrillary tangles and granulovacuolar degeneration in the hippocampus with ageing and dementia. a quantitative study. Acta Neuropathol 1977;37(2):111–8.
Buckner RL, Head D, Parker J, Fotenos AF, Marcus D, Morris JC, et al. A unified approach for morphometric and functional data analysis in young, old, and demented adults using automated atlas-based head size normalization: reliability and validation against manual measurement of total intracranial volume. Neuroimage 2004;23(2):724–38.
Burton EJ, Karas G, Paling SM, Barber R, Williams ED, Ballard CG, et al. Patterns of cerebral atrophy in dementia with levy bodies using voxel-based morphometry. Neuroimage 2002;17:618–30.
Davidson LL, Heinrichs RW. Quantification of frontal and temporal lobe brain-imaging findings in schizophrenia: a meta-analysis. Psychiatry Res 2003;122(2):69–87.
Dickerson BC, Bakkour A, Salat DH, Feczko E, Pacheco J, Greve DN, et al. The cortical signature of Alzheimer's disease: regionally specific cortical thinning relates to symptom severity in very mild to mild ad dementia and is detectable in asymptomatic amyloid-positive individuals. Cereb Cortex 2009;19:497–510.
Fotenos AF, Snyder AZ, Girton LE, Morris JC, Buckner RL. Normative estimates of cross-sectional and longitudinal brain volume decline in aging and AD. Neurology 2005;64:1032–9.
Fox NC, Freeborough PA, Rossor MN. Visualisation and quantification of rates of atrophy in Alzheimer's disease. Lancet 1996;348:94–7.
Giulietti G, Bozzali M, Figura V, Spano B, Perri R, Marra C, et al. Quantitative magnetization transfer provides information complementary to grey matter atrophy in Alzheimer's disease brains. Neuroimage 2012;59:1114–22.
Glei DA, Landau DA, Goldman N, Chuang YL, Rodriguez G, Weinstein M. Participating in social activities helps preserve cognitive function: an analysis of a longitudinal, population-based study of the elderly. Int J Epidemiol 2005;34(4):864–71.
Goldberger AL, Amaral LA, Hausdorff JM, Ivanov P, Peng CK, Stanley HE. Fractal dynamics in physiology: alterations with disease and aging. Proc Natl Acad Sci U S A 2002;99(Suppl. 1):2466–72.
Good CD, Johnsrude IS, Ashburner J, Henson RN, Friston KJ, Frackowiak RS. A voxel-based morphometric study of ageing in 465 normal adult human brains. Neuroimage 2001;14:21–36.
Hamalainen A, Tervo S, Grau-Olivares M, Niskanen E, Pennanen C, Huuskonen J, et al. Voxel-based morphometry to detect brain atrophy in progressive mild cognitive impairment. Neuroimage 2007;37:1122–31.
Im K, Lee JM, Seo SW, Hyung Kim S, Kim SI, Na DL. Sulcal morphology changes and their relationship with cortical thickness and gyral white matter volume in mild cognitive impairment and Alzheimer's disease. Neuroimage 2008a;43:103–13.
Im K, Lee JM, Seo SW, Yoon U, Kim ST, Kim YH, et al. Variations in cortical thickness with dementia severity in Alzheimer's disease. Neurosci Lett 2008b;436:227–31.
King RD, Brown B, Hwang M, Jeon T, George AT. Fractal dimension analysis of the cortical ribbon in mild Alzheimer's disease. Neuroimage 2010;53:471–9.
Kochunov P, Mangin JF, Coyle T, Lancaster J, Thompson P, Riviere D, et al. Age-related morphology trends of cortical sulci. Hum Brain Mapp 2005;26:210–20.
Liebovitch LS. Fractals and chaos simplified for the life sciences. New York: Oxford University Press; 1997.
Liu T, Lipnicki DM, Zhu W, Tao D, Zhang C, Cui Y, et al. Cortical gyrification and sulcal spans in early stage Alzheimer's disease. PLoS ONE 2012;7(2):e31083.
Luders E, Narr KL, Thompson PM, Rex DE, Jancke L, Steinmetz H, et al. Gender differences in cortical complexity. Nat Neurosci 2004;7:799–800.
Marcus DS, Wang TH, Parker J, Csernansky JG, Morris JC, Buckner RL. Open access series of imaging studies (oasis): cross-sectional MRI data in young, middle aged, nondemented, and demented older adults. J Cogn Neurosci 2007;19:1498–507.
Pham TD. Regularity dimension of sequences and its application to phylogenetic tree reconstruction. Chaos Solitons Fractals 2012;45:879–87.
Pincus SM. Approximate entropy as a measure of system complexity. Proc Natl Acad Sci U S A 1991a;88:2297–301.
Pincus SM. Approximate entropy as a measure of system complexity. Proc Natl Acad Sci U S A 1991b;88(6):2297–301.
Richman JS, Moorman JR. Physiological time-series analysis using approximate entropy and sample entropy. Am J Physiol Heart Circ Physiol 2000;278:H2039–49.
Rogan S, Lippa CF. Alzheimer's disease and other dementias: a review. Am J Alzheimers Dis Other Demen 2002;17:11–7.
Sandu AL, Rasmussen IAJ, Lundervold A, Kreuder F, Neckelmann G, Hugdahl K, et al. Fractal dimension analysis of MR images reveals grey matter structure irregularities in schizophrenia. Comput Med Imaging Graph 2008;32:150–8.
Shi F, Liu B, Zhou Y, Yu C, Jiang T. Hippocampal volume and asymmetry in mild cognitive impairment and Alzheimer's disease: meta-analyses of MRI studies. Hippocampus 2009;19:1055–64.
Sluimer JD, van der Flier WM, Karas GB, Fox NC, Scheltens P, Barkhof F, et al. Whole-brain atrophy rate and cognitive decline: longitudinal MR study of memory clinic patients. Radiology 2008;248:590–8.
Spulber G, Niskanen E, Macdonald S, Kivipelto M, Padilla DF, Julkunen V, et al. Evolution of global and local grey matter atrophy on serial MRI scans during the progression from MCI to AD. Curr Alzheimer Res 2012;9:516–24.
Stern Y. What is cognitive reserve? Theory and research application of the reserve concept. J Int Neuropsychol Soc 2002;8(3):448–60.
The Lund and Manchester Groups. Clinical and neuropathological criteria for frontotemporal dementia. J Neurol Neurosurg Psychiatry 1994;57:416–8.
Thompson PM, Hayashi KM, de Zubicaray G, Janke AL, Rose SE, Semple J, et al. Dynamics of gray matter loss in Alzheimer's disease. J Neurosci 2003;23:994–1005.
Toulopoulou T, Grech A, Morris RG, Schulze K, McDonald C, Chapple B, et al. The relationship between volumetric brain changes and cognitive function: a family study on schizophrenia. Biol Psychiatry 2004;56(6):447–53.
Van Essen DC. A tension-based theory of morphogenesis and compact wiring in the central nervous system. Nature 1997;385(6614):313–8.
Welker W. Why does cerebral cortex fissure and fold? a review of determinants of gyri and sulci. Cereb Cortex 1990;8:3–136.
Whitwell JL, Przybelski SA, Weigand SD, Knopman DS, Boeve BF, Petersen RC, et al. 3D maps from multiple MRI illustrate changing atrophy patterns as subjects progress from mild cognitive impairment to Alzheimer's disease. Brain 2007;130:1777–86.
Williams GP. Chaos theory tamed. Washington, DC: Joseph Henry Press; 1997.
Wu YT, Shyu KK, Jao CW, Wang ZY, Soong BW, Wu HM, et al. Fractal dimension analysis for quantifying cerebellar morphological change of multiple system atrophy of the cerebellar type (MSA-C). Neuroimage 2010;49:539–51.
Zhang L, Butler AJ, Sun CK, Sahgal V, Wittenberg GF, Yue GH. Fractal dimension assessment of brain white matter structural complexity post stroke in relation to upper-extremity motor function. Brain Res 2008;1228:229–40.
Zhang Y, Brady M, Smith S. Segmentation of brain MR images through a hidden Markov random field model and the expectation-maximization algorithm. IEEE Trans Med Imaging 2001;20(1):45–57.